Intrinsic Profiles beyond the Capillary Wave Theory: A Monte Carlo Study

E. Chacón[1] and P. Tarazona[2,3]
[1]Instituto de Ciencia de Materiales de Madrid, Consejo Superior de Investigaciones Científicas, Cantoblanco, E-28049 Madrid, Spain
[2]Departamento de Física Teórica de la Materia Condensada, Universidad Autónoma de Madrid, E-28049 Madrid, Spain
[3]Instituto Nicolás Cabrera, Universidad Autónoma de Madrid, E-28049 Madrid, Spain

(Received 5 June 2003; published 16 October 2003)

We develop and test an operational definition of the intrinsic surface for liquid-vapor interfaces. The application to the microscopic configurations along Monte Carlo computer simulations gives the statistical properties of the intrinsic surfaces and the intrinsic density profiles for simple fluid models. The results open a framework of quantitative description to close the gap between the mesoscopic capillary wave theory and the sharpest level of resolution for the intrinsic density distribution, relative to the first atomic layer in the liquid surface, as done in the interpretation of experimental x-ray reflectivity.

DOI: 10.1103/PhysRevLett.91.166103 PACS numbers: 68.03.Hj, 61.30.Hn, 68.03.Kn

The description of the liquid-vapor interface through a smooth density profile, $\rho(z)$, goes back to van der Waals, but the delocalization of the free liquid surface by long wavelength capillary waves (CW) sets a problem in the statistical interpretation of $\rho(z)$, tied to the appearance of long-range surface fluctuations. The capillary wave theory (CWT) [1–3] incorporates these fluctuations by means of an *intrinsic surface*, $z = \xi(\mathbf{R}) = \sum_q \hat{\xi}_q e^{i\mathbf{q}\cdot\mathbf{R}}$, to represent the instantaneous microscopic boundary between liquid and vapor, at each transverse position $\mathbf{R} = (x, y)$. For large $R_{12} = |\mathbf{R}_1 - \mathbf{R}_2|$, the two-particle distribution function is represented by the average over the intrinsic surface shapes of two *intrinsic profiles*, $\tilde{\rho}(z)$, shifted by the local values of $\xi(\mathbf{R})$,

$$\rho^{(2)}(z_1, z_2, R_{12}) \approx \langle \tilde{\rho}[z_1 - \xi(\mathbf{R}_1)]\tilde{\rho}[z_2 - \xi(\mathbf{R}_2)]\rangle.$$

The *microscopic* structure in the perpendicular direction is included through $\tilde{\rho}(z)$, while the long-ranged transverse dependence goes with the intrinsic surface correlations, $\langle \xi(\mathbf{R}_1)\xi(\mathbf{R}_2)\rangle$. The two key assumptions of the CWT are that $\tilde{\rho}(z)$ and $\xi(\mathbf{R})$ are statistically uncorrelated, and that the later follows a simple surface Hamiltonian leading to uncorrelated Gaussian probabilities for each Fourier component and $\langle |\hat{\xi}_q|^2\rangle = (\beta\gamma_o A q^2)^{-1}$, with the macroscopic surface tension $\beta\gamma_o$, in $k_B T = 1/\beta$ units. The finite transverse size $A \equiv L_x^2$ enters through the lower limit of the wave vector, with periodic boundary conditions $q \geq 2\pi/L_x$, while the fixed number of particles, N, restricts the fluctuations of the $\hat{\xi}_0$ component. The specific definition of $\xi(\mathbf{R})$ and, in particular, the upper limit $q_u \geq q$ for the level of resolution at which $\xi(\mathbf{R})$ follows the atomic positions, would determine the shape of the intrinsic profile [2],

$$\tilde{\rho}(z, q_u) = \left\langle \frac{1}{A}\sum_{i=1}^{N} \delta(z - z_i + \xi(\mathbf{R}_i))\right\rangle. \tag{1}$$

The link between CWT and the density functional (DF) or other microscopic theories for the liquid-vapor density profile $\rho(z)$ [4,5] has not been established at a quantitative level because of the uncertainty in the separation of "bulk" and "surface" fluctuations, tied to the choice of q_u and the shape of $\tilde{\rho}(z)$. Qualitatively it is expected that q_u should not go beyond $2\pi/\sigma$, in terms of the molecular diameter σ, and that $\tilde{\rho}(z)$ is a rather sharp function, since the CWT gives the density profile, with transverse size L_x, as the smoother Gaussian convolution:

$$\rho(z, L_x) = \int dz' \frac{\tilde{\rho}(z', q_u)}{\sqrt{2\pi\Delta_{CW}}} \exp\left(-\frac{(z - z')^2}{2\Delta_{CW}}\right), \tag{2}$$

with the CW square width $\Delta_{CW}(L_x, q_u) = \sum_q \langle \hat{\xi}_q^2\rangle$.

Mecke and Dietrich [5] used a DF approximation to check the validity of the CWT assuming that $\tilde{\rho}(z)$ is the DF profile for a planar surface, without explicit dependence on q_u. Such a smooth intrinsic profile removed problems associated to a step function $\tilde{\rho}(z)$ [6], but still the nonlocal molecular interactions reduced the validity of the macroscopic surface Hamiltonian to values of q_u well below $2\pi/\sigma$. On the other hand, the analysis of x-ray reflectivity data for liquid metals Hg [7] and Ga [8,9] [which showed layering structures in $\rho(z, L_x)$, for $L_x \sim 10^3$ Å] makes use of the CWT with the assumption that the intrinsic profile is a delta function followed by a strongly oscillatory structure, similar to that of the distribution function $g(r)$ in the bulk liquid [7]. Using Δ_{CW} in (2) as a free parameter to transform the delta function of $\tilde{\rho}(z)$ into a Gaussian first peak in $\rho(z, L_x)$, and to fit the experimental reflectivity data, drowns together the lack of a precise value for L_x and the arbitrariness in q_u. In previous works [10,11], we have analyzed Monte Carlo (MC) results for simple fluid models which share the low ratio between triple and critical temperatures, T_t/T_c, of Hg and show structured surfaces. The deconvolution of those $\rho(z, L_x)$ to putative CWT intrinsic profiles [11], with $q_u = 2\pi/\sigma$, showed a strongly structured $\tilde{\rho}(z)$, but still far from being a delta function.

The use of such different assumptions and results for the shape of $\tilde{\rho}(z)$ reflects the lack of connection between the CWT and a truly microscopic view of the liquid surfaces. In this Letter, we explore this question with the *direct* evaluation of $\xi(\mathbf{R})$ and $\tilde{\rho}(z)$ along MC simulations for simple fluid models, to get both the statistical distribution of the intrinsic surface and the shape of the intrinsic profiles, as functions of q_u. The MC simulations are done with the soft-alkali (SA) model [11], at several temperatures clearly above its triple point ($T_t/T_c = 0.1$), using 2592 particles in periodic boundary rectangular boxes, with $L_x = L_y \approx 9\sigma$ and $L_z \approx 81\sigma$, initialized with a liquid slab (of thickness around 27σ) with upper and lower interfaces normal to the z direction. The high values of $\beta\gamma_o$ (Table I) reduce the amplitude of the capillary waves and make our L_x large enough to reach the range of the CWT. For comparison, we present results for the Lennard-Jones (LJ) system, for which L_x is not large enough to reach the validity of the CWT, as observed with larger size simulations [12].

A *local* Gibbs dividing surface, as definition of $\xi(\mathbf{R})$, had been used in MC simulations to study the CW effects in polymer mixtures [13] but, to avoid the damping of the surface structures by bulk fluctuations, we searched for a definition of the intrinsic surface tied directly to a set of pivot atoms at each surface of the liquid slab. For each sampling configuration, we use a percolative criterion to eliminate the particles in the vapor [14] and select as (upper and lower) initial sets of nine pivots the most external atomic positions in a mesh of prisms with transverse size $L_x/3 \approx 3\sigma$. The initial intrinsic surface is defined as the minimal area surface going through all the pivots and restricted to have Fourier components with $|\mathbf{q}| \leq q_m$. Then we add as new pivots those particles which are closer to $\xi(\mathbf{R})$ than a prefixed distance τ, and recalculate a new $\xi(\mathbf{R})$ until self-consistency is reached.

TABLE I. Thermodynamic parameters in our MC simulations, for the soft-alkali (SA) and Lennard-Jones (LJ) models. $\Delta_{CW}(L_x, q_u)$ is the MC result for the CW mean square amplitude, $\delta a_i = a_i - \tilde{a}_i - \Delta_{CW}$ give the correlation effects for the thickening of the first Gaussian layers ($i = 0, 2$), and $\delta z_{01} = \delta z_0 - \delta z_1$ for the distance between the first two layers, all with atomic diameter σ units.

	T/T_c	$\beta\gamma_o$	L_x	δa_0	δa_1	δa_2	δz_{01}	Δ_{CW}
SA								
	0.15	8.23	9.02	0.039	0.024	0.006	0.036	0.041
	0.21	5.34	9.06	0.058	0.037	0.014	0.038	0.053
	0.33	2.97	9.16	0.100	0.073	0.061	0.089	0.072
LJ								
	0.63	0.93	9.78	0.356	0.173	0.041	0.200	0.165

For each microscopic configuration we obtain in this way the intrinsic surface and the set of N_p pivots lying on it, $\xi(\mathbf{R}_i) = z_i$. From (1), the averaged intrinsic profiles, $\tilde{\rho}(z, q_m)$ shown by the lowest curves in Fig. 1, contain delta-function first peaks (shown as arrows), with two-dimensional densities (arrows height) given by the mean number of pivots per unit area, $\langle N_p \rangle/A$, followed by layered structures which resemble the density profiles for liquids near planar walls. We fix the parameter τ from the stability of $\tilde{\rho}(z)$ with respect to it; for too low τ, the peak at $z \approx \sigma$ develops a shoulder just beyond the cutoff $z = \tau$, while for τ above an upper threshold the number of pivots grows unbounded, as $\xi(\mathbf{R})$ becomes corrugated and merges into the bulk. The optimal values are $\tau \approx 0.5\sigma$, well within the intuitive meaning of this parameter, to separate the intrinsic surface from the *inner* particles. We take $q_m = 16\pi/L_x \sim 2\pi/\sigma$, which implies using 193 $\hat{\xi}_q$ components, to fit the z positions of around 60 pivots. With a much lower q_m, the number of variables approaches the number of pivots, the requirement of $\xi(\mathbf{R})$ being a minimal area surface becomes irrelevant, and the *overfitting* effect increases the squared amplitudes $|\hat{\xi}_q|^2$; if q_m is too large, $\xi(\mathbf{R})$ develops wedges between pivots, and $|\hat{\xi}_q|^2$ are depleted, although $\tilde{\rho}(z)$ changes very little.

No CWT assumption is made to get these intrinsic surfaces and profiles; $\xi(\mathbf{R})$ may bend around the pivot

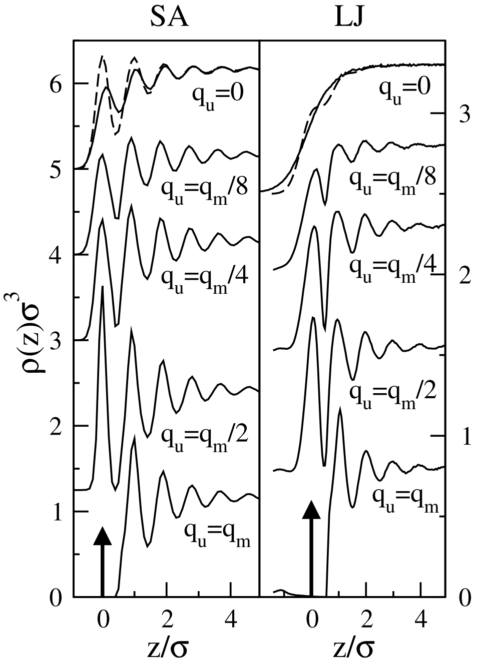

FIG. 1. Intrinsic profiles, $\tilde{\rho}(z, q_u)$, in units of the atomic diameter σ, for the SA at $T/T_c = 0.15$, and the LJ at $T/T_c = 0.63$; the curves for different q_u are displaced vertically. The dashed lines at the top give the CWT convolution of the intrinsic profiles at the bottom, with the mean square displacement of the intrinsic surface, Δ_{CW} , obtained in our simulations.

particles in a much sharper way than what would be reasonably described with a macroscopic surface Hamiltonian [6], and the intrinsic profile is not required to be statistical independent of $\xi(\mathbf{R})$. The validity of the CWT would be reached with smoother intrinsic surfaces, keeping only the Fourier components of $\xi(\mathbf{R})$ with $|\mathbf{q}| \leq q_u < q_m$. With this restriction on the short wavelength fluctuations of the intrinsic surface, $\xi(\mathbf{R})$ would not go precisely through the positions of the pivot particles, and the intrinsic profiles $\tilde{\rho}(z, q_u)$ in Fig. 1 have increasingly broader peaks as q_u decreases. If $q_u < 2\pi/L_x$, then $\xi(\mathbf{R}) = \hat{\xi}_0$, and the result of (1) becomes similar to the plain density profiles $\rho(z, L_x)$, since the flat intrinsic surface is similar to the Gibbs dividing surface described by the center of mass and the total number of particles.

The averaging over 10^4 configurations, separated by 50 MC steps, shows uncorrelated Gaussian distributions for the Fourier components $\hat{\xi}_q$ of the intrinsic surface, which are described in Fig. 2 by the value of $\langle|\hat{\xi}_q|^2\rangle$ or equivalently by the q dependent surface tension, $\gamma(q) \equiv (\beta A q^2 \langle|\hat{\xi}_q|^2\rangle)^{-1}$ used in [5]. For the stiff surface of the SA model at the lowest T, the CWT assumption $\gamma(q) \approx \gamma_o$ is valid for $q\sigma \leq 2$; beyond this range $\gamma(q)$ grows and produces the gradual (but faster than CWT) damping of the CW. Increasing T reduces the region with $\gamma(q) \approx \gamma_o$, and for the LJ fluid our simulation box is not large enough to reach the CWT limit. Despite their different values of $\beta\gamma_o$, all the values of $\beta\gamma(q)$ for $q\sigma > 2$ are roughly similar, producing the common (apparently exponential) decay of $|\hat{\xi}_q|^2$, in clear contrast with the CWT assumption $|\hat{\xi}_q|^2 = (\beta\gamma_o A q^2)^{-1}$.

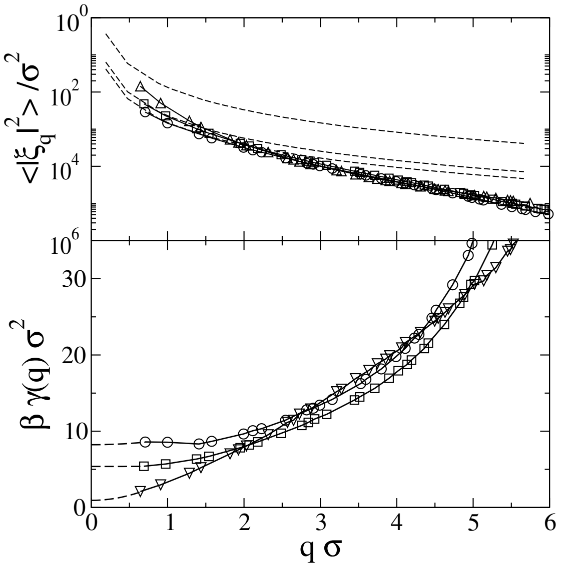

FIG. 2. The mean squared amplitude of the intrinsic surface Fourier components and the effective q-dependent surface tension, $\gamma(q)$, in $k_B T$ and atomic diameter σ units. Circles: SA at $T/T_c = 0.15$; squares: SA at $T/T_c = 0.21$; triangles: LJ at $T/T_c = 0.63$. The low q values of $\gamma(q)$ are extrapolated (broken lines) to the macroscopic surface tension γ_o. The dashed lines in the upper graph give the CWT predictions.

For the coldest SA surface, the three upper intrinsic profiles in Fig. 1 (left) are within the CWT range. Although damped with respect to that for q_m, they preserve the oscillatory layering structure. In contrast, the oscillations of $\tilde{\rho}(z, q_m)$ for the LJ model are fully damped, top curve of Fig. 1 (right), before reaching the range of $\gamma(q) \approx \gamma_o$. This is consistent with the proposal of Mecke and Dietrich [5] of a smooth (DF-like) shape for $\tilde{\rho}(z)$, rather than a sharp step function, which would not be reproduced by any of our $\tilde{\rho}(z, q_m)$. The much sharper view of the liquid surface with a delta-function description of the first liquid layer, assumed in the analysis of the x-ray reflectivity, is certainly beyond the range of validity of the CWT. Nevertheless, our procedure to locate $\xi(\mathbf{R})$ in each microscopic configuration shows that such $\tilde{\rho}(z, q_m)$ exist, as a natural description of the interface at the sharpest possible microscopic level. Near the critical temperature, the method would lead to unnatural shapes for $\tilde{\rho}(z, q_m)$ and strong dependence with the parameter τ, as the separation between the first atomic layer and the inner liquid would be artificial for very rough surfaces and low liquid densities. However, the application near the triple point of simple (LJ-like) liquids seems to be justified, since the shapes of $\tilde{\rho}(z, q_m)$ are natural and robust with respect to the choice of τ and q_m.

The direct generalization of the CWT to include the effective $\gamma(q)$ obtained in our MC simulations fails to reproduce the MC density profiles $\rho(z, L_x)$, from the Gaussian convolution (2) of $\tilde{\rho}(z, q_m)$ (dashed lines at the top of Fig. 1). The failure comes from the correlation between the roughness of $\xi(\mathbf{R})$, for a given configuration, and its contribution to $\tilde{\rho}(z)$; the atomic correlations, together with our operational definition of intrinsic surface, lead to the accumulation of pivots at the maxima and minima of $\xi(\mathbf{R})$, so that the mean square deviation of the pivots' z coordinate is larger than the mean square deviation of $\xi(\mathbf{R})$ [15]. This is reflected in the first peak of the intrinsic profiles in Fig. 1; within the CWT the gradual incorporation of the CW effects should lead (from bottom to top) to similar increments for the square width of each peak, while our microscopic evaluation of $\tilde{\rho}(z, q_u)$ shows a much faster broadening of the first peak.

To include the correlation between $\xi(\mathbf{R})$ and the atomic positions requires a nontrivial extension of the CWT. At low temperatures, we may use the *distorted crystal* parametrization used for the interpretation of x-ray reflectivity experiments [7], and in our previous analysis of $\rho(z, L_x)$ [10,11]. The intrinsic density profile is assumed to be a series of Gaussian peaks, describing atomic layers of two-dimensional density $\tilde{n}_i$, mean position $\tilde{z}_i$, and square width $\tilde{a}_i$, with a delta-function first peak when $\tilde{\rho}(z)$ is pushed to the sharpest resolution,

$$\tilde{\rho}(z) = \tilde{n}_0 \delta(z) + \sum_{i=1}^{\infty} \frac{\tilde{n}_i}{\sqrt{2\pi \tilde{a}_i}} \exp\left[-\frac{(z - \tilde{z}_i)^2}{2\tilde{a}_i} \right]. \qquad (3)$$

The number of free parameters is reduced by setting, for $i \geq 4$, linear increases $\tilde{a}_{i+1} = \tilde{a}_i + \alpha$, $\tilde{z}_{i+1} = \tilde{z}_i + \zeta$, and $\tilde{n}_i = \rho_o \zeta$ in terms of the bulk liquid density ρ_o, while the vapor density is neglected. The CWT prediction for $\rho(z, L_x)$, using this intrinsic profile parametrization in (2), would have the same functional form (3) but with square widths $a_i = \tilde{a}_i + \Delta_{\mathrm{CW}}$, increased by the CW contribution as it would result from (2). We may now use these functional forms for $\tilde{\rho}(z, q_{\mathrm{m}})$ and $\rho(z, L_x)$ to fit our MC results for the intrinsic and the averaged density profiles, restricted to have identical layers densities ($\tilde{n}_i \equiv n_i$), and equal values of α and ζ for both density profiles, but taking $\tilde{a}_i$ and a_i as independent parameters for $i \leq 3$. The correlation effects beyond the CWT in each layer would be given by $\delta a_i \equiv a_i - \tilde{a}_i - \Delta_{\mathrm{CW}}$. To get a good fit to both profiles, we have also to allow the free variation in the position of the first layers (i.e., using $\delta z_i = \tilde{z}_i - z_i$ as independent fitting parameters). The results, in Table I, show that at very low temperatures the correlation effect is reduced to the first layers. For the LJ model, the effects appear well inside the liquid phase, but still we may get a good common fit to $\tilde{\rho}(z, q_{\mathrm{m}})$ and $\rho(z, L_x)$ with a few parameters to describe the deviation from the CWT.

In conclusion, we have shown that an operational definition of intrinsic surface may be used in MC simulations to obtain intrinsic density profiles of liquid surfaces, with atomic layering structures similar to that of dense fluid near walls. The method has been applied not only to a liquid-metal model, with $T_t/T_c \approx 0.1$, for which the layering had been directly observed in MC density profiles $\rho(z, L_x)$, but also at the higher temperature of the LJ liquid. The shape of the intrinsic profiles depends strongly (bottom to top curves of Fig. 1) on wavelength cutoff assumed for the fluctuations of the intrinsic surface, q_{u}.

Our MC results validate the assumptions of the CWT up to a very short wavelength of the corrugation ($q_{\mathrm{u}} \approx \pi/\sigma$) for cold liquids, in agreement with the analysis of experimental results [7,8]. The dependence with q_{u} below this range would just represent the standard CWT arbitrariness in the separation of bulk and surface fluctuations, and tied to the value of Δ_{CW} in (2). However, our intrinsic profiles for these values of q_{u} are qualitatively similar to those of the DF approximations rather than to the step function assumed in some theoretical analysis or the delta-function peaks used to interpret the x-ray reflectivity results. We observe that the limit of validity for the CWT depends strongly on T, which for the LJ model of a simple fluid is reached only when the intrinsic profile has become monotonic, in contrast with the oscillatory $\tilde{\rho}(z, q_{\mathrm{u}})$ for liquid-metal models.

Within our scheme, we may go to a sharper level of description for the liquid interface, and get the delta-function first peak in $\tilde{\rho}(z, q_{\mathrm{m}})$, using an intrinsic surface corrugated up to wavelength of molecular size ($q_{\mathrm{m}} \approx 2\pi/\sigma$). However, this requires an extension of the CWT with a wave vector dependent surface tension $\gamma(q)$ and the correlation between the intrinsic profiles and surfaces. This extension allows the prediction of the density profile, averaged over any transverse window size L_x, in terms of $\tilde{\rho}(z, q_{\mathrm{m}})$, $\gamma(q)$, and a few parameters to describe the correlation effect in the first liquid layers. The implication of this CWT extension for the interpretation of the x-ray diffraction data and other experimental proves of the liquid surfaces requires further analysis, and the connection of $\tilde{\rho}(z, q_{\mathrm{u}})$ with the density profiles obtained within the DF formalism should also be explored; hopefully the direct determination of $\xi(\mathbf{R})$ and $\tilde{\rho}(z, q_{\mathrm{u}})$ in computer simulations, as presented here, may open a quantitative framework of description for liquid surfaces, closing the gap between the mesoscopic CWT and the microscopic DF theories.

This work has been supported by the Dirección General de Investigación (MCyT) of Spain, under Grant No. BFM2001-1679-C03.

---

[1] F. P. Buff, R. A. Lovett, and F. H. Stillinger, Phys. Rev. Lett. **15**, 621 (1965).

[2] J. K. Percus and G. O. Williams, in *Fluid Interfacial Phenomena*, edited by C. A. Croxton (Wiley, New York, 1986), pp. 1–44.

[3] J. Penfold, Rep. Prog. Phys. **64**, 777 (2001).

[4] R. Evans, in *Fundamentals of Inhomogeneous Fluids*, edited by D. Henderson (Dekker, New York, 1992), pp. 85–175; J. S. Rowlinson and B. Widom, *Molecular Theory of Capillarity* (Clarendon, Oxford, 1982).

[5] K. R. Mecke and S. Dietrich, Phys. Rev. E **59**, 6766 (1999), and references therein.

[6] M. Napiórkowshi and S. Dietrich, Phys. Rev. E **47**, 1836 (1993).

[7] O. Magnussen *et al.*, Phys. Rev. Lett. **74**, 4444 (1995); E. DiMasi *et al.*, Phys. Rev. B **58**, R13 419 (1998).

[8] M. Regan *et al.*, Phys. Rev. Lett. **75**, 2498 (1995).

[9] H. Tostmann *et al.*, J. Non-Cryst. Solids **250–252**, 182 (1999).

[10] E. Chacón *et al.*, Phys. Rev. Lett. **87**, 166101 (2001).

[11] P. Tarazona *et al.*, J. Chem. Phys. **117**, 3941 (2002); E. Velasco *et al.*, J. Chem. Phys. **117**, 10 777 (2002).

[12] S.W. Sides, G. S. Grest, and M.-D. Lacasse, Phys. Rev. E **60**, 6708 (1999).

[13] A. Werner, F. Schmid, M. Müller, and K. Binder, J. Chem. Phys. **107**, 8175 (1997).

[14] The pivots are selected among the particles with at least $\nu = 3$ neighbors, closer than $d = 1.5\sigma$, in the cluster spanning the full slab. At low T, the results are quite robust with respect to ν and d.

[15] The use of local normal coordinates, as in Ref. [5], may partially incorporate some of these correlation effects, but it makes much more cumbersome the relationship between $\tilde{\rho}(z, q_{\mathrm{u}})$ and $\rho(z, L_x)$.